Tellus (1999), 51A, 937–950
Printed in UK.

TELLUS
ISSN 0280–6495

Ice crystal habits and solar radiation

By KLAUS WYSER*, *Department of Meteorology, Stockholm University, 106 91 Stockholm, Sweden*

(Manuscript received 15 September 1998; in final form 6 April 1999)

ABSTRACT

The single-scattering properties of cirrus clouds depend not only upon the ice water path and the size of the crystals, but also upon the crystal shape. A novel parameterization has been used to explore the differences in broadband short-wave radiation due to various crystal habits. The differences in the net-fluxes are found to be appreciable, both at the tropopause and at the surface. They reach values up to the order of several 10 W m^{-2} for mid-latitude and up to some 100 W m^{-2} for tropical cirrus. The largest differences are found for an intermediate range of optical depths and the optical thickness of natural cirrus happen to be in this intermediate range. The absorptivity of the cirrus cloud is independent of the crystal habit, nevertheless, the change in the cloud's reflectivity has an impact on the tropospheric absorption and, thus, the energy absorbed by the troposphere depends on the crystal habit. The sensitivity of the results with respect to surface albedo and solar zenith angle has been investigated. A lower zenith angle enhances the differences found for the various habits, and this effect is even amplified by a high amount of water vapour as it may be found in the tropics. A comparison with observations from ICE'89 reveals that the large differences in the modelled fluxes are comparable to the uncertainty in the measurements. Despite this observational difficulty, the large differences in SW fluxes emphasise the importance of the crystal habit for radiation schemes.

1. Introduction

Cirrus clouds are important for the Earth's climate as they interact with long- and short-wave (SW) radiation (Liou 1986). They directly affect the reflectivity and absorptivity of the atmosphere, and various feedback may lead to even larger effects on the energy balance. A number of studies found a high sensitivity in the response of large-scale models to the assumptions or parameterizations used for cirrus clouds (Stephens et al., 1990; Liou and Takano, 1994; Sinha and Shine, 1994; Lohmann and Roeckner, 1995). Despite all these efforts, cirrus are still poorly understood and many questions connected with their representation in large-scale models (e.g., GCMs) remain unanswered. The present work puts its focus on just one aspect of all the questions related to cirrus, namely the differences in SW radiation due to various crystal habits.

A major problem in the calculation of the radiative fluxes is the non-sphericity of ice crystals. Analytical solutions are known for the scattering and absorption of radiation by spherical particles. On the other hand, the interaction of radiation with non-spherical particles has no analytic solution in general except for a special geometry of the particle (Liou and Takano, 1994). Approximate solutions have been developed to find the single-scattering properties for individual ice crystals (Stephens et al., 1990; Liou and Takano, 1994; Macke et al., 1996). Large-scale models do not treat the interaction of radiation with each crystal but use the bulk radiative properties of cirrus instead. They are obtained by combining the single-scattering properties for individual crystals

* Present address: Institute for Computational Earth System Science, UCSB, Santa Barbara, CA 93106-3060, USA.
e-mail: klaus@icess.ucsb.edu

with appropriate size distributions. The bulk radiative properties are often related to bulk cloud variables in large-scale models in order to derive appropriate parameterizations.

The simplest parameterization links the optical properties to the ice water content (IWC) only (Rockel et al., 1991; Sun and Shine, 1994; Platt, 1997). However, several studies have demonstrated that the optical properties depend on the size of the ice crystals as well (Stephens et al., 1990; Fu and Liou, 1993). In general, the reflectivity of a cloud with small particles is higher than with large particles for the same ice water path. Parameterizations for the single-scattering properties of clouds have been developed that besides the IWC also depend on the "mean" crystal size (Ebert and Curry, 1992; Francis et al., 1994; Fu, 1996; Mitchell et al., 1996). The "mean" crystal size is often denoted as effective size or radius, but, unfortunately, the definition for the effective radius is not unambiguous for non-spherical crystals (Wyser, 1998).

Parameterizations for ice clouds have been derived under the assumption of hexagonal columns for the crystal habit (Ebert and Curry, 1992; Fu, 1996). The extinction coefficient and the single-scattering albedo (ω) are independent of the particle shape in the geometric optics regime (Fu, 1996). On the other hand, the asymmetry parameter (g, a measure for the difference in the forward and backward scattered energy) strongly depends on the crystal shape. The phase function for any given particle, and thus g, can in principle be found with ray-tracing techniques (Takano and Liou, 1995; Macke et al., 1996; Yang and Liou, 1996, 1997). However, the demand for computer resources is appreciable as time consuming Monte Carlo computations have to be repeated for each size and shape of the particles and for each wavelength.

Wyser and Yang (1998) employed an improved geometric optics method to calculate the single-scattering properties for ice crystals from seven different habits: solid and hollow columns, plates, bullet rosettes, aggregates, needles, and spheres. The bulk single-scattering properties for ice clouds were found by combing the results with various size distributions. Finally, a parameterization has been derived that expresses the single-scattering properties of cirrus clouds in terms of ice water path, average crystal size, and crystal habit.

The objective of the present work is to investigate the sensitivity of the SW radiative fluxes to the various crystal habits. The question is if the SW radiation scheme of large-scale models should account for the various crystal habits. Several studies have been published that examine the differences in optical properties between various crystal shapes (Iaquinta et al., 1995; Chervet et al., 1996; Macke et al., 1996). However, all these studies are limited to visible wavelengths and a generalisation of their findings for broadband SW fluxes is not possible as the absorption coefficient for ice has large variations in the near infrared.

Kinne and Liou (1989) compared the radiative effects of ice spheres and hexagonal crystals. They found an albedo difference of up to 10% depending on the optical thickness (τ) and solar zenith angle. This albedo difference is equivalent to a difference in the net cloud forcing at the top of the atmosphere of 40 W m^{-2} for a Cs and of 15 W m^{-2} for a Ci cloud, with $\tau = 1$ in both clouds. In a Ci cloud with $\tau = 10$ the difference in net forcing exceeds 50 W m^{-2} for low zenith angles.

Mitchell et al. (1996) have derived a parameterization for the optical properties of several crystal habits. Calculating the albedo with observed mean crystal size they find differences of up to 20% between columns and bullet rosettes for identical ice water path. The differences to plates and planar polycrystals are smaller. The large difference between columns and bullet rosettes appears puzzling compared to the good agreement found by Wyser and Yang (1998) for this two habits. The reason for this are the different definitions for the average size: the mean size used by Mitchell et al. (1996) is not identical to the average size in the sense of Wyser and Yang (1998). Hence, a quantitative comparison of the results from Mitchell et al. (1996) with the present work is not possible. Nevertheless, it is interesting to note the substantial albedo differences for the different habits.

The present work is organised as follows. Section 2 gives an overview of the radiation scheme and the parameterization for the single-scattering properties of ice clouds. The radiation scheme is then used in Subsection 3.1 to calculate the radiative transfer in two clouds observed during ICE'89 to compare calculated and measured fluxes. The differences in SW radiation between the various habits are systematically investigated in Subsection 3.2 for a typical cirrus cloud. Subsection 3.3 examines the sensitivity of the findings to changes in the ambient conditions. The possible impact for climate modelling is described in Subsection 3.4 and the conclusions in Section 4 summarise the results from this study and discuss implications for large-scale models.

2. Radiation model

The one-dimensional short-wave radiation scheme is a four-band two-stream scheme comparable to those used in advanced GCMs (Savijärvi et al., 1997). It takes into account gaseous Rayleigh scattering (as in Ritter and Geleyn (1992)), water vapour absorption by a k-distribution method, based on Ramaswamy and Freidenreich (1992), and stratospheric ozone absorption (Savijärvi, 1990). Clouds are described by their single-scattering properties optical thickness (τ), single-scattering albedo (ω), and asymmetry parameter (g). The transmissivity and absorptivity of a single cloudy layer is calculated with a δ-Eddington scheme (Slingo, 1989). The layers are then added by taking into account multiple reflections (Liou, 1992).

The radiative properties of ice clouds depend on the ice water path (IWP) and the average size of the ice crystals (D_a). The average size is defined as

$$D_a = \frac{V}{P}, \tag{1}$$

where V is the total ice volume and P the total projected area of the crystals. The single-scattering properties become independent of the details of the size distribution if the average size is defined by (1) (Wyser and Yang, 1998). A similar definition for a mean size has been suggested by Foot (1998) and Fu (1996). It is straightforward to relate V to the ice water content of the cloud, but no method of relating P to ambient conditions has been developed so far. Fu (1996) has applied his definition of a generalized effective size (D_{ge}) to observed size distributions from several field experiments; using (1) as the definition for the average size yields D_a between 15 and 113 μm with a median of 47 μm. However, the values given by Fu are based on the assumption that all ice crystals are hexagonal columns. As no general method exists yet how to relate the crystal habit to other cloud variables, it is chosen to prescribe D_a for the present study.

Wyser and Yang (1998) have developed a parameterization for the single-scattering properties of ice crystals:

$$\tau = \frac{\mathrm{IWP}}{\rho_{ice}} \left(\frac{a_1}{D_a} + a_0 \right), \tag{2}$$

$$\omega = \sum_{i=0}^{2} b_i D_a^i, \tag{3}$$

$$g = \sum_{i=0}^{2} c_i D_a^i, \tag{4}$$

where $\rho_{ice} = 916.7\ \mathrm{kg\,m^{-3}}$ is the bulk density of ice. The parameterization is valid for D_a in the range between 20 and 100 μm. Values for the coefficients a_i, b_i, and c_i may be found in Wyser and Yang (1998). The optical thickness and the single-scattering albedo are independent of the crystal shape in the geometric optics limit (Fu, 1996). The phase function and thus g depends on the habit and, hence, the set of c_i is different for each habit.

The radiation scheme calculates up- and downward SW fluxes, $S^{\uparrow}$ and $S^{\downarrow}$, respectively, and the net flux at any level becomes

$$S^{net} = S^{\downarrow} - S^{\uparrow}. \tag{5}$$

The absorption of SW radiation in a given layer is equivalent to the flux convergence. In a two-stream scheme, it becomes

$$A = S^{net}(\mathrm{top}) - S^{net}(\mathrm{bottom}), \tag{6}$$

where top and bottom denote the boundaries of the layer under consideration. The absorption of the whole troposphere will be denoted as A^{tr}. The heating rate of a layer is given by

$$\frac{\partial T}{\partial t} = \frac{g' A}{c_p[p(\mathrm{bottom}) - p(\mathrm{top})]} = \frac{g'[S^{net}(\mathrm{top}) - S^{net}(\mathrm{bottom})]}{c_p[p(\mathrm{bottom}) - p(\mathrm{top})]}, \tag{7}$$

where g' is the acceleration of gravity, c_p the heat capacity at constant pressure, and p the pressure at the upper and lower boundary of the layer, respectively.

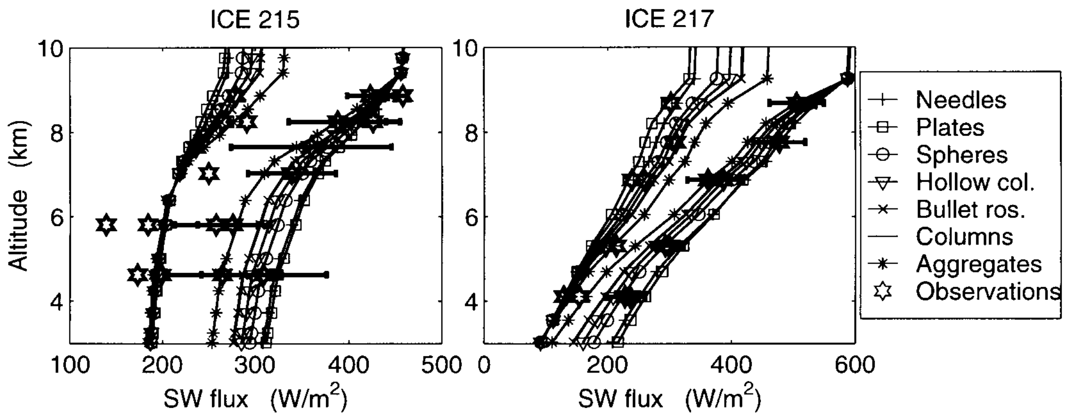

Fig. 1. Observed and modelled SW fluxes from ICE'89. The solar zenith angles are 68.3 (ICE 215) and 62.2 (ICE 217). The standard deviations for the measured $S^{\uparrow}$ are omitted for better legibility.

3. Results

3.1. Observed ice clouds from ICE'89

The microphysical and radiative properties of two selected cirrus clouds were observed during the International Cirrus Experiment (ICE'89, Francis et al., 1994). The flights were made on two days, abbreviated as ICE 215 and ICE 217, respectively. Reasonable agreement was found in an earlier study between the observed solar fluxes and model results obtained with various parameterizations of ice cloud radiative properties (Francis et al., 1994).

The profiles of temperature and humidity described in Francis et al. (1994) are taken to calculate the SW fluxes. The definition for the effective radius (r_e) used by Francis et al. differs from D_a by a constant factor,

$$D_a = \frac{4}{3} r_e. \tag{8}$$

At first, the observed r_e has been adjusted to account for small undetected ice crystals (Francis et al., 1994). The adjusted value is then put into (8) to yield D_a and the single-scattering properties are obtained with (2)–(4). The reported TWC probe value for IWC (IWCT in Francis et al.) is used here to calculate IWP.

High values for r_e were reported at the lowest cloud level, outside the range for which the parmeterization (2)–(4) is valid. It is not justified to simply use an upper limit for D_a as this would lead to an overestimated optical thickness of the lowest cloud layer. Instead, a maximum value of 100 μm is taken for D_a and, at the same time, IWC is reduced accordingly while conserving the ice crystal number density. The suggested correction takes the form

$$\mathrm{IWC_{corr}} = \mathrm{IWC}\left(\frac{\min(100\ \mu\mathrm{m},\ D_a)}{D_a}\right)^3, \tag{9}$$

where the assumption has been made that the crystal concentration is proportional to $\mathrm{IWC}/\mathrm{D}_a^3$. The reduction of IWC underestimates the cloud absorption, but this is considered to be of minor importance as the absorptivity of clouds is much smaller than their reflectivity.

The calculated and observed SW fluxes are shown in Fig. 1. Note that the upward fluxes have been adjusted to the observations to account for reported but not closely observed water clouds below the cirrus. A similar adjustment was used by Francis et al. (1994) in their comparisons. The modelled $S^{\downarrow}$ and $S^{\uparrow}$ are within the standard deviation of the observations for all cloud layers with the exception of the lowest layers during ICE 217. It should be noted, however, that the standard deviation was quite large, especially during ICE 215. The prescribed upward flux at the surface makes a surface albedo unnecessary. Using a surface albedo instead would enhance the impact of the various habits on the upward fluxes as the differences in the cloud transmittance would be accounted for twice. The highest transmissivity is

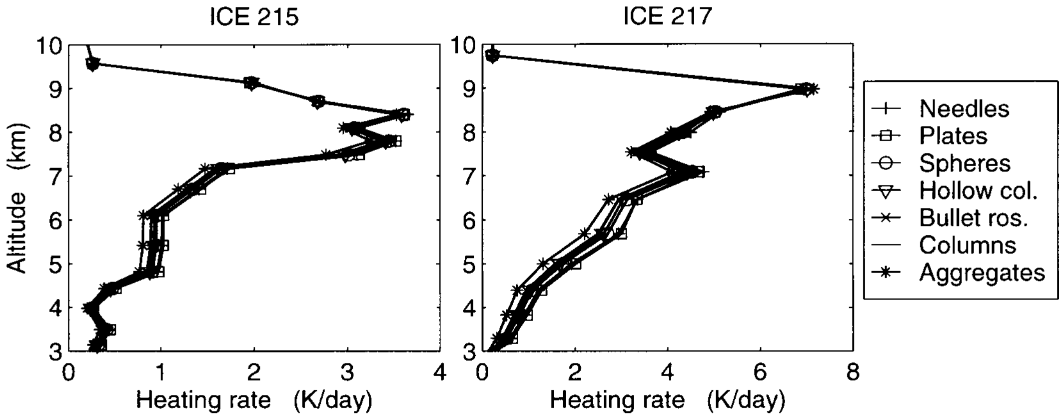

Fig. 2. Computed heating rates for ICE'89.

found for clouds consisting of plates whereas aggregates transmit least. Reflectivity and transmissivity are complimentary since the absorption is almost independent of the habit (see below). Therefore, clouds with aggregates have the highest reflectivity and those with plates the lowest. Note however that despite the differences in reflectivity, most radiation is scattered in the forward direction for any habit.

Fig. 2 shows the calculated heating rates. They agree with the results of Francis et al. (1994) in the upper, but not in the lower part of the cloud. The discrepancy arises from the IWC correction introduced by (9) that reduces the absorption in the lowest cloud layer. Such a reduction is thus not to recommend for studies of cloud dynamics. From the figure, it follows that the heating rates are not very different for the various crystal habits even though the fluxes vary substantially. In particular the strongest heating rate near the cloud top is equal for all habits. The parameterization for ω is independent of the habit and, subsequently, the absorption is almost independent as well except for a small contribution originating from differences in the reflectivity.

Three conclusions can be drawn from the comparison with the data from ICE'89.

- The radiative fluxes differ for the various crystal habits, however, the variation is in the range of the observational uncertainty. Therefore, it is not possible to infer the crystal habits from the measured fluxes during ICE 215 and ICE 217.
- The net radiative fluxes at the surface or at the top of the atmosphere depends on the crystal habit, the differences between the various habits are on the order of several 10 W m^{-2}.
- The computed heating rates differ only slightly between the various habits and the impact of the habits on cloud dynamics is presumably low.

The clouds from ICE'89 with high IWP and vertical extension of several kilometres are untypical compared to average cirrus cloud properties (Dowling and Radke, 1990). Nevertheless, the comparison with observations shows that the parameterization (2)–(4) yields reasonable radiative fluxes.

3.2. *Model study of a typical cirrus cloud*

The previous section demonstrated that the various crystal habits may lead to substantial differences in the radiative fluxes. To study the impact of the habits more systematically, a setup for a typical cirrus cloud is defined. Radiative fluxes are calculated for clouds that are identical except for the crystal habit, in particular, the average size is equal for all habits. The net SW fluxes at the tropopause and at the surface as well as the absorption in the whole troposphere and in the cloud are compared. The sensitivity of the results to changes in the assumed cirrus cloud parameters will be investigated in Subsection 3.3.

In all experiments, the cirrus cloud is centered at 10 km altitude with a geometrical thickness of 1 km. The average size D_a is chosen as 40 μm, equivalent to $r_e = 30$ μm according to the definition of Francis et al. (1994). The IWC is varied between 10^{-3} and 10 g m^{-3} which covers the range of observed cirriform clouds (Heymsfield, 1993). The mid-latitude temperature and humidity profiles are taken from McClatchey et al. (1972) but in-cloud relative humidity is set to 100%. The solar zenith angle is 60° and the surface albedo 0.1.

Fig. 3 displays the results obtained with the radiation scheme as a function of IWP. Frames (a) and (b) show S^{net} at the tropopause and at the surface, respectively. The differences due the various crystal habits are largest for intermediate IWP between 10 and 1000 g m^{-2}. For lower IWP the habits are not important as the cloud is highly transparent. For higher IWP the cloud becomes opaque and the differences in S^{net} vanish at the surface. Nevertheless, the cloud albedo remains sensitive to the crystal habit even for high IWP. Of all the habits considered, needles reflect least sunlight back to space while the reflectivity is highest for aggregates. The maximum difference in S^{net} between aggregates and needles reaches 130 W m^{-2} at the tropopause and 100 W m^{-2} at the surface. Table 1 lists S^{net} and A^{tr} for the various habits for a cloud with IWP = 100 g m^{-2} as an example. The difference in S^{net} between any two habits exceeds some 10 W m^{-2} in general. This is important for the energy budget at the surface as S^{net} is the amount of absorbed energy. Not taking into account the crystal habit might induce an appreciable systematic error in large-scale models. It is also evident from Table 1 that the SW radiation absorbed in the troposphere differs for the various habits although the differences are smaller than those for the net fluxes.

The radiation is absorbed in the troposphere by the cloud itself and by other constituents, mainly water vapour. From Fig. 3c follows that the absorption increases with IWP. Moreover, the higher the reflectivity of the cirrus cloud, the lower the absorption in the troposphere as a larger fraction of the downward radiation is reflected back to space from the cloud top and does not reach lower layers. The largest difference in A^{tr} is found between needles and aggregates, it is about 30 W m^{-2} for IWP $\geqslant$ 200 g m^{-2}. The difference is significant compared to the clear-sky absorption of 110 W m^{-2} and, thus, the absorption of radiation in the troposphere is considered to be sensitive to the crystal habit. A local maximum appears in Fig. 3c around IWP = 300 g m^{-2}. This maximum is due to the fact that atmospheric absorption takes place simultaneously in the ice cloud and the water vapour below the cloud. The water vapour absorption decreases with increasing IWP, but at the same time the absorption by the ice crystals increases. The maximum appears where the reduction of the water vapour absorption due to higher reflectivity outweighs the increase in the cloud absorptivity.

Table 1. *Net SW radiation (W m^{-2}) at the tropopause and at the surface for the typical cirrus defined in Subsection 3.2 with IWP = 100 g m^{-2}; also shown is the SW absorption in the troposphere*

	S^{net} tropopause	S^{net} surface	A^{tr}
needles	424.0	287.6	136.4
plates	405.9	273.2	132.7
spheres	385.4	257.5	127.9
hollow col.	358.4	235.3	123.1
bullet ros.	341.0	221.3	119.7
columns	339.5	220.2	119.3
aggregates	304.1	192.1	112.0

Fig. 3d shows the cloud absorption is independent of the habit for low IWP. Differences become apparent for IWP above 200 g m^{-2} and reach about 30 W m^{-2} between aggregates and needles for IWP $\geqslant$ 1000 g m^{-2}. The IWP in natural cirrus is often lower than that and the impact of the different crystal habits on the cloud heating rate is considered to be unimportant.

The comparison of frames (c) and (d) in Fig. 3 reveals an interesting difference between the radiative flux convergence in the troposphere and in the cloud layer only. The absorption in the whole troposphere depends on the habit even for low IWP, but this is not the case for the in-cloud absorption. The absorption in the whole troposphere is the sum of the absorption by the cloud and by water vapour. Since cirrus clouds are located high in the troposphere, there is an appreciable amount of water vapour below the cloud. The absorptivity in the cloud does not change with the habit, but the transmissivity does. The absorption of radiation by water vapour below the cloud depends on the radiation that reaches the subcloud layer and, subsequently, A^{tr} depends indirectly on the optical properties of the cloud.

3.3. *Sensitivity experiments*

The preceding section describes how the different crystal habits alter the radiative fluxes in a

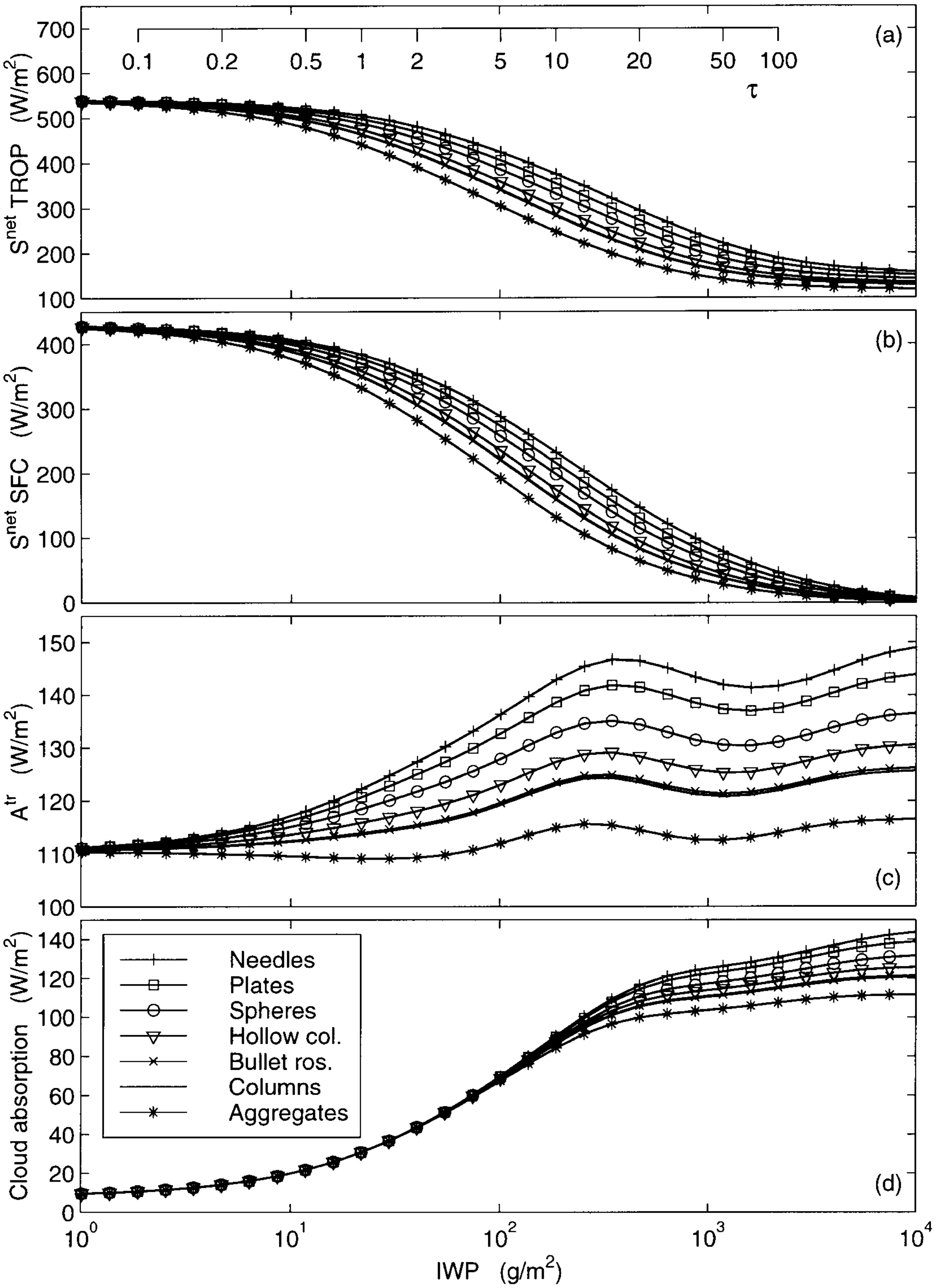

Fig. 3. Net SW fluxes, tropospheric and in-cloud absorption for the cirrus cloud defined in Subsection 3.2. The inset in frame (a) shows the optical depth calculated with (2).

typical cirrus cloud. Obviously, the results depend on the assumptions that have been used to define the cirrus. This section will investigate the sensitivity of S^{net} to changes in the average size, the surface albedo, and the solar zenith angle.

The SW cloud forcing is defined as $\text{SCF} = S^{\text{net}} - S_0^{\text{net}}$ where S_0^{net} is the clear-sky net SW flux. In general, SCF is evaluated in large-scale models over a certain time, and diurnal or seasonal cycles are averaged. The integration with time also allows for feedback mechanisms to dampen or amplify the effects of clouds so that the real effect of clouds for the climate is obtained. The one-dimensional radiation model used in this study yields the instantaneous forcing instead without any time integration or feedback processes. Therefore, a different measure for the impact of the crystal habits is suggested here, namely the maximum difference in S^{net} for any habit relative to spheres:

$$\Delta S^{\text{net}} = \max_{\text{IWP}}(S^{\text{net}} - S^{\text{net}}_{\text{spheres}}). \tag{10}$$

The maximum in (10) is taken while varying IWP between 10 and 10^4 g m^{-2} (Fig. 4). The comparison against spheres is arbitrary, any other habit could be chosen as well. However, a motivation for spheres is the fact that many radiation schemes use ice spheres to calculate the radiative transfer in ice clouds, and the present study may give an indication of how much the possible impact of the change to another habits might be. The difference ΔS^{net} is a measure for the maximum difference that may result from a wrong assumption of the crystal habit. Alternatively, it can be interpreted as the maximal radiative forcing induced by the change from spheres to any other habit,

$$\max_{\text{IWP}} \Delta\,\text{SCF} = \max_{\text{IWP}}(\text{SCF} - \text{SCF}_{\text{spheres}}) = \Delta S^{\text{net}}, \tag{11}$$

since S_0^{net} is independent of the habit. The difference between ΔS^{net} for any two habits, say needles and aggregates, is then a measure of how much the net fluxes might differ between these two habits. Dividing ΔS^{net} by S_0^{net} defines the normalised difference.

3.3.1. Crystal size. The pattern of S^{net} displayed in Fig. 3a does not change qualitatively while varying D_a (Fig. 5a). However, the region with the largest differences due to the various habits moves towards lower IWP for $D_a = 20$ μm and in the opposite direction for $D_a = 80$ μm. The shift of the pattern while varying D_a is related to the change of the optical thickness given by (2). Plotting S^{net} as a function of τ instead of IWP removes the differences originating from the variation in D_a (Fig. 5b). The largest differences in S^{net} are found for τ in the range between approximately 2 and 30.

Table 2 lists ΔS^{net} for different crystal sizes. The habits can be classified in three groups according to their response to a size change relative to the response for spheres. Needles and aggregates change in the same way as spheres and ΔS^{net} is

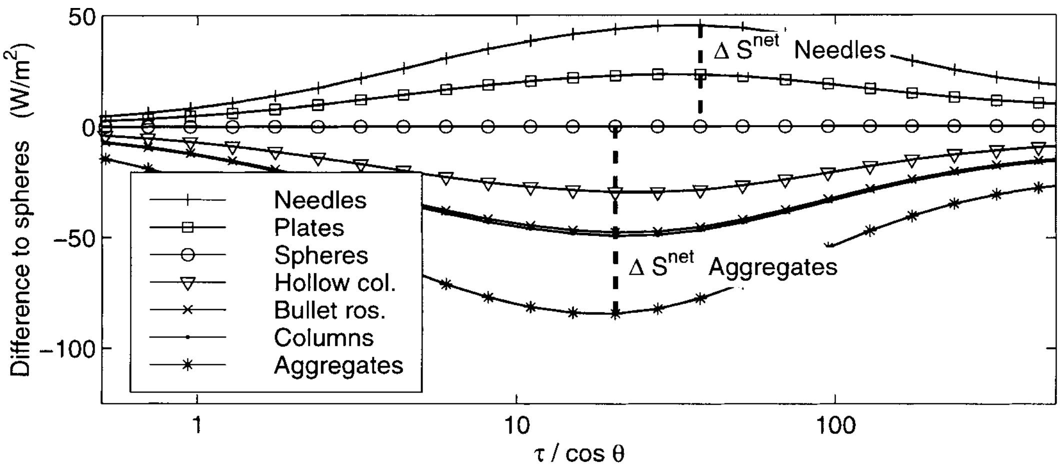

Fig. 4. The definition of the maximum difference ΔS^{net}.

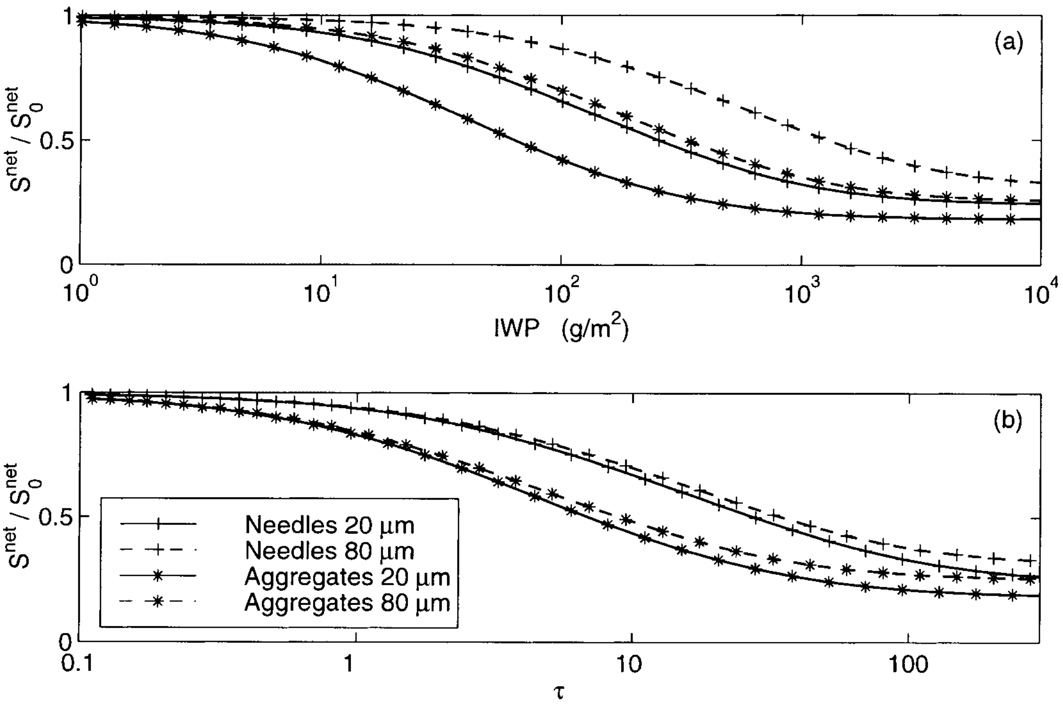

Fig. 5. Normalised net flux at tropopause as a function of IWP and τ for two values of D_a. Shown are only results for needles and aggregates.

Table 2. *Sensitivity of the net flux differences to changes in the average size*

	$D_a = 20$ μm		$D_a = 40$ μm		$D_a = 80$ μm	
	ΔS^{net}	$\Delta S^{net}/S_0^{net}$	ΔS^{net}	$\Delta S^{net}/S_0^{net}$	ΔS^{net}	$\Delta S^{net}/S_0^{net}$
			Tropopause			
needles	46.9	0.09	45.5	0.08	34.4	0.06
plates	−14.8	−0.03	23.4	0.04	56.5	0.10
hollow cols.	−42.8	−0.08	−29.4	−0.05	−17.3	−0.03
bullet ros.	−58.7	−0.11	−47.6	−0.09	−36.4	−0.07
columns	−60.7	−0.11	−49.1	−0.09	−37.7	−0.07
aggregates	−82.1	−0.15	−84.3	−0.16	−83.8	−0.15
			Surface			
needles	36.0	0.08	34.4	0.08	27.3	0.06
plates	−12.9	−0.03	17.2	0.04	43.2	0.10
hollow cols.	−35.2	−0.08	−23.9	−0.06	−14.1	−0.03
bullet ros.	−48.0	−0.11	−38.2	−0.09	−29.0	−0.07
columns	−49.5	−0.11	−39.3	−0.09	−29.9	−0.07
aggregates	−66.8	−0.16	−67.0	−0.16	−65.2	−0.15

Listed are the maximum flux differences (ΔS^{net} (W m^{-2})) between the habits of the first column and spheres; the differences are also normalised with the clear-sky net flux S_0^{net}.

Table 3. *As Table 2 but for a variation of the surface albedo*

	Alb = 0.05		Alb = 0.1		Alb = 0.2	
	ΔS^{net}	$\Delta S^{net}/S_0^{net}$	ΔS^{net}	$\Delta S^{net}/S_0^{net}$	ΔS^{net}	$\Delta S^{net}/S_0^{net}$
			Tropopause			
needles	47.1	0.08	45.5	0.08	42.2	0.08
plates	24.3	0.04	23.4	0.04	21.8	0.04
hollow cols.	−30.7	−0.05	−29.4	−0.05	−27.1	−0.05
bullet ros.	−49.6	−0.09	−47.6	−0.09	−43.8	−0.09
columns	−51.1	−0.09	−49.1	−0.09	−45.1	−0.09
aggregates	−87.5	−0.16	−84.3	−0.16	−77.8	−0.16
			Surface			
needles	36.4	0.08	34.4	0.08	30.3	0.08
plates	18.2	0.04	17.2	0.04	15.2	0.04
hollow cols.	−25.3	−0.06	−23.9	−0.06	−21.2	−0.06
bullet ros.	−40.3	−0.09	−38.2	−0.09	−33.8	−0.09
columns	−41.4	−0.09	−39.3	−0.09	−34.8	−0.09
aggregates	−70.9	−0.16	−67.0	−0.16	−59.2	−0.15

not affected by a change in D_a. Needles with $D_a = 80\ \mu m$ are an exception as the parameterization (2)–(4) reaches its limit of validity for such large needles. For columns, both solid and hollow, and bullet rosettes ΔS^{net} is reduced when D_a increases. Finally, plates do not belong to neither of the two other classes as ΔS^{net} increases for larger D_a.

3.3.2. Surface albedo. Increasing the surface albedo from 0.05 to 0.2 reduces ΔS^{net} as listed in Table 3. On the other hand, the normalised $\Delta S^{net}/S_0^{net}$ do not depend on the albedo. Thus, the change in the albedo affects the clear-sky and the cloud net fluxes in the same way, independent of the crystal habit. This means that the reason for the change in ΔS^{net} is the change in the clear-sky net flux, the different crystal habits in the cloud neither amplify nor dampen the effects from the albedo change.

3.3.3. Solar zenith angle. The pattern of S^{net} shown in Fig. 3a does not change while varying θ, but it is stretched along the IWP-axis (Fig. 6a). In the case with variable D_a, the translation of the pattern was compensated for by using τ instead of IWP. Similarly, the differences in the pattern for various θ are greatly reduced if S^{net} is plotted versus $\tau/\cos\theta$ (Fig. 6b). The largest differences in S^{net} between the various habits are found for $\tau/\cos\theta$ in the approximate range $5 \leqslant \tau/\cos\theta \leqslant 50$.

Table 4 lists the variation of ΔS^{net} with the zenith angle. The differences between the various habits are reduced when θ increases, both the absolute and the normalised values. The change in ΔS^{net} is partly caused by the change in the incoming solar radiation, partly by the change in the reflectivity of the cloud.

3.4. *Impact for climate modelling*

Three different atmospheric profiles (temperature and humidity) are taken from McClatchey et al. (1972) to study the possible impact of the crystal habit for climate modelling purposes. The solar zenith angle is chosen differently for the three profiles:

TRO	tropical	$\theta = 0^\circ$
MLS	mid-latitude summer	$\theta = 40^\circ$
SAW	sub-arctic winter	$\theta = 75^\circ$

Surface albedo is 0.1 and the average size $D_a = 40\ \mu m$. The cirrus cloud is located around 10 km altitude in all three cases, geometrical cloud thickness is 1 km and in-cloud relative humidity is 100%. The differences in the temperature profiles are not important as scattering and absorption of SW radiation are independent of the temperature. Water vapour on the other hand is a strong absorber of SW radiation and, hence, the differences in the humidity profiles are expected to be more important.

Table 5 lists ΔS^{net} for the three atmospheric

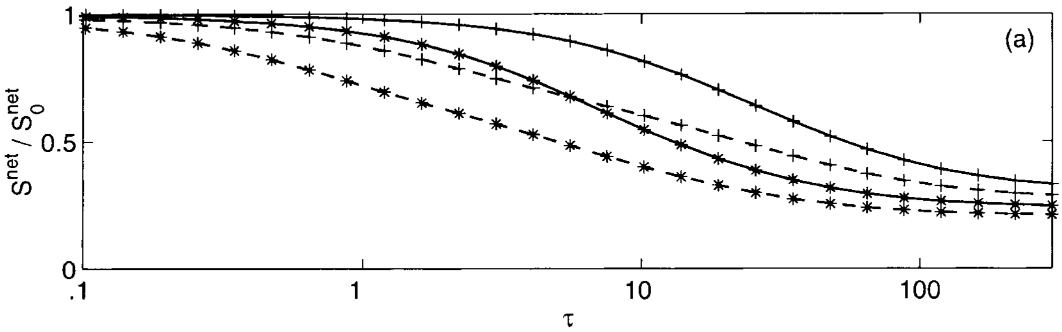

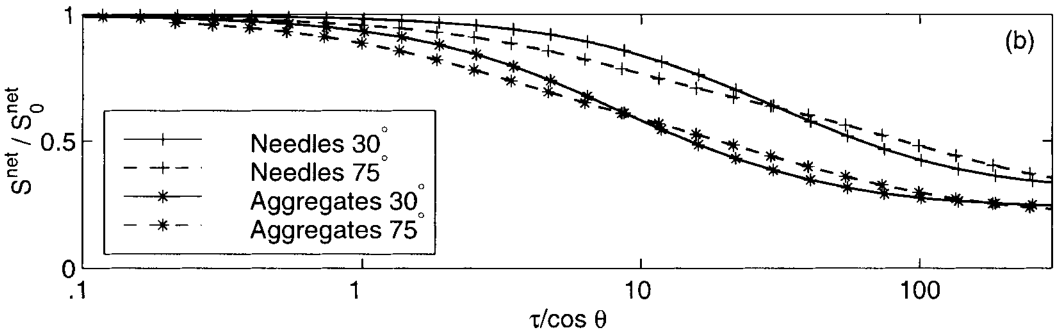

Fig. 6. Normalized net flux as a function of τ and $\tau/cos\ \theta$. Shown are only results for needles and aggregates.

Table 4. *As Table 2 but for a variation of the solar zenith angle*

	$\theta = 30°$		$\theta = 60°$		$\theta = 75°$	
	ΔS^{net}	$\Delta S^{net}/S_0^{net}$	ΔS^{net}	$\Delta S^{net}/S_0^{net}$	ΔS^{net}	$\Delta S^{net}/S_0^{net}$
			Tropopause			
needles	96.5	0.10	45.5	0.08	19.1	0.07
plates	49.2	0.05	23.4	0.04	10.0	0.04
hollow cols.	−64.6	−0.07	−29.4	−0.05	−11.9	−0.05
bullet ros.	−103.7	−0.11	−47.6	−0.09	−19.3	−0.07
columns	−106.8	−0.11	−49.1	−0.09	−20.0	−0.08
aggregates	−181.6	−0.18	−84.3	−0.16	−34.5	−0.13
			Surface			
needles	80.7	0.10	34.4	0.08	13.0	0.07
plates	40.9	0.05	17.2	0.04	6.5	0.03
hollow cols.	−55.7	−0.07	−23.9	−0.06	−9.1	−0.05
bullet ros.	−88.5	−0.11	−38.2	−0.09	−14.5	−0.08
columns	−90.9	−0.11	−39.3	−0.09	−14.9	−0.08
aggregates	−155.9	−0.19	−67.0	−0.16	−25.3	−0.13

profiles. Subsection 3.3.3 has shown that the large variation of ΔS^{net} is due to the changes in the zenith angle. However, Tables 4 and 5 are not directly comparable as θ is different in the two tables. The computation has been repeated for the three temperature and humidity profiles, but with zenith angles of 30°, 60°, and 75°, respectively (not shown). The variation due to θ is amplified by the

Table 5. *As Table 2 but for three different atmospheric profiles*

	TRO		MLS		SAW	
	ΔS^{net}	$\Delta S^{net}/S_0^{net}$	ΔS^{net}	$\Delta S^{net}/S_0^{net}$	ΔS^{net}	$\Delta S^{net}/S_0^{net}$
			Tropopause			
needles	117.1	0.10	81.8	0.09	15.3	0.06
plates	59.2	0.05	41.7	0.05	7.6	0.03
hollow cols.	−78.6	−0.07	−54.4	−0.06	−10.6	−0.04
bullet ros.	−126.3	−0.11	−87.1	−0.10	−17.0	−0.07
columns	−130.1	−0.11	−89.7	−0.10	−17.4	−0.07
aggregates	−221.6	−0.19	−153.7	−0.18	−29.7	−0.12
			Surface			
needles	99.0	0.10	66.7	0.09	13.9	0.06
plates	49.9	0.05	33.9	0.05	6.9	0.03
hollow cols.	−68.1	−0.07	−46.0	−0.06	−9.7	−0.05
bullet ros.	−108.9	−0.12	−73.8	−0.10	−15.5	−0.07
columns	−112.0	−0.12	−75.9	−0.11	−15.9	−0.07
aggregates	−189.3	−0.20	−129.2	−0.18	−27.0	−0.13

humidity, that is ΔS^{net} is enhanced for $\theta = 30°$ and reduced for $\theta = 60°$ compared to Table 4.

The largest effects from the various habits are found in the tropics. The combination of low zenith angle and high amounts of sub-cloud water vapour leads to large differences between the various habits. The differences between the various ΔS^{net} are typically on the order of some 10 W m^{-2} and may reach several 100 W m^{-2}. They are smaller at higher latitudes, but still reach some 10 W m^{-2} for the MLS profile. The largest difference between needles and aggregates exceeds 200 W m^{-2} even at mid-latitudes. At high latitudes, the differences between the habits become rather small and are probably not significant for climatic purposes.

4. Conclusions

The single-scattering properties of ice crystals depend on the crystal habit, and, therefore, the interaction between SW radiation and cirrus clouds will depend on the crystal habit as well. A novel parameterization of the single-scattering properties of ice clouds has been used to investigate the impact from the various crystal habits. A comparison of modelled fluxes with observations from ICE'89 reveals that the differences in the SW radiation flux between the various habits are on the order of some 10 W m^{-2}. It is not possible, however, to retrieve the crystal habit from the observed fluxes as the uncertainties in the observations are too large.

The various crystal shapes are less important for optically thin or thick clouds as the differences in the net fluxes vanish at the surface. In an intermediate range of optical thickness, however, S^{net} is found to differ substantially between the various habits. This intermediate range is given by $5 \leqslant \tau/\cos\theta \leqslant 50$ where $\tau/\cos\theta$ is the optical thickness normalised by the solar zenith angle. For a typical cirrus with $D_a = 40$ μm, IWC = 0.05 g m^{-3}, and $\Delta z = 2$ km, the optical thickness becomes $\tau = 5.5$. Hence, natural cirrus are expected to fall in the range where the differences between the various habits are rather large. The differences in S^{net} between the various habits are qualitatively equal at the tropopause and at the surface although the absolute differences are slightly larger at the tropopause.

In general, the cloud absorption is independent of the habit except for very large τ. On the other hand, the differences between the habits in the tropospheric absorption increase with τ to reach a maximum at $\tau/\cos\theta \approx 30$ and remain more or less constant thereafter. The differences between the habits are smaller for A^{tr} than for S^{net}, but, nevertheless, they can be substantial and the energy absorbed in the troposphere may differ by several 10 W m^{-2} depending on the habit.

The results from this study demonstrate the importance of the crystal habits for the calculation of the radiative transfer in large-scale models. The largest differences between the various habits are found in the tropics because of the low zenith angle and the large amount of water vapour below the cloud. Appreciable differences in the SW fluxes of up to some 100 W m^{-2} have been found for a tropical atmosphere. The differences are smaller at higher latitudes but they are still on the order of typically several 10 W m^{-2} for mid-latitude cirrus. A wrong assumption about the crystal habit can lead to a considerable error in the energy budget. The differences in S^{net} are comparable in magnitude to the heat flux at the surface. Errors resulting from a wrong crystal habit might be substantial systematic errors that have to be compensated, for example by flux correction.

The findings from this study, in particular the high magnitude of the differences between the habits, should be interpreted with caution as there are three major caveats. This study only considers solar radiation. An investigation of the long-wave effects from various crystal habits is necessary to see if, possibly, the large differences found in the short-wave fluxes may be offset. Moreover, all results were obtained for overcast sky. The real effect on the climate could be estimated by multiplying them with an averaged cloud cover. However, the maximum differences between the habits are still considerably large even if a cloud cover of only 20% is assumed, in particular in the tropics. Finally, the impact from the various habits has been investigated for fixed zenith angle which was chosen for noon conditions in most cases. Climatological effects are thus expected to be smaller than this instantaneous values as they are averaged over a diurnal cycle.

Another source of uncertainty are feedback processes in the atmosphere. The present work concentrates on the instantaneous SW effects from the different crystal habits. Feedback between radiation, temperature, and humidity may affect the amount of ice and the position of the cloud, but also the average size and the crystal habit. It is not obvious whether feedback mechanisms will enhance or reduce the differences between the various habits.

The present study has demonstrated the appreciable differences in the SW flux arising from various crystal shapes. The high sensitivity emphasises the importance of the crystal habits for solar radiation. It is evident that large-scale models should account for the shape of ice crystals. However, there are two important questions left that have to be answered before the radiative effects from the different crystal habits can be used in practice: what is the average size of the crystals and what habits are present in a cirrus for which only temperature and ice content are known? These issues require further investigations in order to develop appropriate parameterizations for the crystal habits and average sizes in large-scale models.

5. Acknowledgements

I would like to thank Professor H. Sundqvist for the help and discussions while preparing the manuscript, and Dr. P. Francis who kindly provided the data from ICE'89. This study has been supported by the Swedish Natural Science Council (NFR) under grant G-AA/GU02923-323}.

REFERENCES

Chervet, P., H. Isaka and T. Nakajima, 1996. Influence of crystal shapes on radiative fluxes in visible wavelength: ice crystals randomly oriented in space. *Ann. Geophys.* **14**, 837–844.

Dowling, D. R. and F. L. Radke, 1990. A summary of the physical properties of cirrus clouds. *J. Appl. Meteor.* **29**, 970–978.

Ebert, E. E. and J. A. Curry, 1992. A parameterization of ice cloud optical properties for climate models. *J. Geophys. Res.* **97**, 3831–3836.

Foot, J. S. 1988. Some observations of the optical properties of clouds (II). Cirrus. *Quart. J. Roy. Meteor. Soc.* **114**, 145–164.

Francis, P. N., A. Jones, R. W. Saunders, K. P. Shine, A. Slingo and Z. Sun, 1994. An observational and theoretical study of the radiative properties of cirrus: Some results from ICE'89. *Quart. J. Roy. Meteor. Soc.* **120**, 809–848.

Fu, Q. 1996. An accurate parameterization of the solar radiative properties of cirrus clouds for climate models. *J. Climate* **9**, 2058–2082.

Fu, Q. and K. N. Liou, 1993. Parameterization of the radiative properties of cirrus clouds. *J. Atmos. Sci.* **50**, 2008–2025.

Heymsfield, A. J., 1993. Microphysical structures of stratiform and cirrus clouds. In: P. V. Hobbs (ed.), *Aerosol–cloud–climate interactions*, vol. 54, *International Geophysics Series*, pp. 97–121. Academic Press.

Iaquinta, J., H. Isaka and P. Personne, 1995. Scattering phase function of bullet rosette ice crystals. *J. Atmos. Sci.* **52**, 1401–1413.

Kinne, S. and K. N. Liou, 1989. The effects of the nonsphericity and size distribution of ice crystals on the radiative properties of cirrus clouds. *Atmos. Res.* **24**, 273–284.

Liou, K. N. 1986. Influence of cirrus clouds on weather and climate processes: A global perspective. *Mon. Wea. Rev.* **114**, 1167–1199.

Liou, K. N., 1992. *Radiation and cloud processes in the atmosphere*. Oxford University Press, 487 pp.

Liou, K. N. and Y. Takano, 1994. Light scattering by nonspherical particles: Remote sensing and climatic implications. *Atmos. Res.* **31**, 271–298.

Lohmann, U. and E. Roeckner, 1995. Influence of cirrus cloud radiative forcing on climate and climate sensitivity in a general circulation model. *J. Geophys. Res.* **100**, 16305–16323.

Macke, A., J. Mueller and E. Raschke, 1996. Single scattering properties of atmospheric ice crystals. *J. Atmos. Sci.* **53**, 2813–2825.

McClatchey, R. A., R. W. Fenn, J. E. A. Selby, F. E. Volz and J. W. Garing, 1972. *Optical properties of the atmosphere*, 3rd edition. Air Force Cambridge Research Laboratories.

Mitchell, D. L., A. Macke and Y. Liu, 1996. Modeling cirrus clouds. Part II: Treatment of radiative properties. *J. Atmos. Sci.* **53**, 2967–2988.

Platt, C. M. R. 1997. A parameterization of the visible extinction coefficient of ice clouds in terms of ice/water content. *J. Atmos. Sci.* **54**, 2083–2098.

Ramaswamy, V. and S. M. Freidenreich, 1992. A study of broadband parametrizations of the solar radiative interactions with water vapor and water drops. *J. Geophys. Res.* **97**(D11), 11487–11512.

Ritter, B. and J. F. Geleyn, 1992. A comprehensive radiation scheme for numerical weather prediction models with potential applications in climate simulations. *Mon. Wea. Rev.* **120**, 303–325.

Rockel, B., E. Raschke and B. Weynes, 1991. A parameterization of broad band radiative transfer properties of water, ice and mixed phase clouds. *Beitr. Phys. Atmosph.* **64**, 1–12.

Savijärvi, H. 1990. Fast radiation parameterization schemes for mesoscale and short-range forecast models. *J. Appl. Meteor.* **29**, 437–447.

Savijärvi, H., A. Arola and P. Räisänen, 1997. Shortwave optical properties of precipitating waterclouds. *Quart. J. Roy. Meteor. Soc.* **123**, 883–899.

Sinha, A. and K. P. Shine, 1994. A one-dimensional study of possible cirrus cloud feedbacks. *J. Climate* **7**, 158–173.

Slingo, A. 1989. A GCM parameterization for the shortwave radiative properties of water clouds. *J. Atmos. Sci.* **46**, 1419–1427.

Stephens, G. L., S.-C. Tsay, P. W. Stackhouse, Jr. and P. J. Flatau, 1990. The relevance of the microphysical and radiative properties of cirrus clouds to climate and climatic feedback. *J. Atmos. Sci.* **47**, 1742–1753.

Sun, Z. and K. P. Shine, 1994. Studies of the radiative properties of ice and mixed-phase clouds. *Quart. J. Roy. Meteor. Soc.* **120**, 111–137.

Takano, Y. and K. N. Liou, 1995. Radiative transfer in cirrus clouds. Part III: Light scattering by irregular crystals. *J. Atmos. Sci.* **52**, 818–837.

Wyser, K. 1998. The effective radius in ice clouds. *J. Climate* **11**, 1793–1802.

Wyser, K. and P. Yang, 1998. Average ice crystal size and bulk short-wave single-scattering properties of cirrus clouds. *Atmos. Res.* **49**, 315–335.

Yang, P. and K. N. Liou, 1996. Geometric-optics-integral-equation method for light scattering by nonspherical ice crystals. *Appl. Opt.* **35**, 6568–6584.

Yang, P. and K. N. Liou, 1997. Light scattering by hexagonal ice crystals: Solutions by ray-by-ray integration algorithm. *J. Opt. Soc. Am. A* **14**, 2278–2289.